Chapter 1

The Global and Regional Climate System

by Hans von Storch

Abstract

The relationships between planetary and regional or local scales of the climate system are discussed.
The main features of the planetary scale climate may be understood as the response of the climate system to the planetary scale forcing (heating by the sun), the distribution of continents and largest mountain ranges. The regional climate, then, may be understood as the result of both the planetary scale climate and the regional features such as secondary mountains, marginal seas, land use, and the like.
The small scale features have little effect on the planetary scale in the sense that *details* are rather unimportant; but the statistics of the small scale features modify the planetary scale state significantly. This modification may be described by parameterizations, i.e., through statistics of small scale processes, which are *conditioned* by the large-scale states.
The concept of randomized parameterizations is introduced.
The discourse is illustrated with various examples, ranging from energy balance models, the emergence of the general circulation of the atmosphere from a state at rest to downscaling applications.

1.1 Prologue

Seen as a resource or limiting factor, climate is a local or regional object. In areas where temperatures fall below the freezing point, palm trees do not grow, and the agronomist is advised not grow citrus trees. Therefore, not surprisingly, climatology as a science began with the description of local and regional climates, and the various regional charts were combined in world maps. In that sense, the global climate was perceived as the sum of regional climates. Famous representatives of this line of research are Vladimir Köppen, Eduard Brückner or Julius von Hann. Köppen's (1923) maps are even nowadays famous; they classify the surface of the world into climatic zones, which are determined by the amount of precipitation they receive, and the temperature regime. Dynamical quantities such as the wind are considered secondary who deserve attention mostly since they determine the primary variables, namely precipitation and temperature. For demonstration, we reprint one of Köppen's maps in Figure 1.1.

The weather services pursue this traditional line of research, by providing "climate normals" for planning exercises in traffic, agriculture, tourism, and other applications. Such normals do not only refer to mean values derived from, say, a 30 year interval, but also the probability for extreme events (such as 100-year storm surges).

On the other hand, a different line of reasoning has developed in the course of centuries – aimed at the understanding why climate is as it is. Examples of research of this type are George Hadley's explanation of the trade wind system[1] (see Figure 1.2), and Emanuel Kant's postulation of a continent south of the Indonesian archipelago – at that time unknown – based on wind observations from merchant vessels. In the same category is Arrhenius (1896) hypothesis about the impact of air-borne carbon dioxide on near-surface temperature.

The two views have long been separated, and are re-conciliated now after the emergence of "global warming", which has its societal implications on the local and regional scale, but which prospect was born in the global realm of climate dynamics.

A major progress of climate research is the understanding that the local climate is only partially determined by local features, such as geographical locations, local topography, proximity to the ocean, land use and the like. Globally averaged features are defined as the arithmetic mean of many local features - but with the help of *energy balance models* these averaged quantities, such as the global mean *near-surface temperature*[2], can be determined directly without knowledge about any local aspects (Section 1.2). Also, the major features of the general circulation of the atmosphere, such as the tropical meridional cells, the jet streams associated with baroclinic instability

[1] For an interesting review of the history of ideas concerning the general circulation of the atmosphere, of which the trade wind system is part of, refer to Lorenz (1967).

[2] With this expression we mean the globally averaged air temperature at 2m height.

Figure 1.1: One of Vladimir Köppen's climate maps of the world. The figure caption is in German.

Figure 1.2: Hadley's concept of thermally driven vertical cells, which are deflected by the rotation of the earth, creating the equator-ward directed trade winds. From Lorenz (1967)

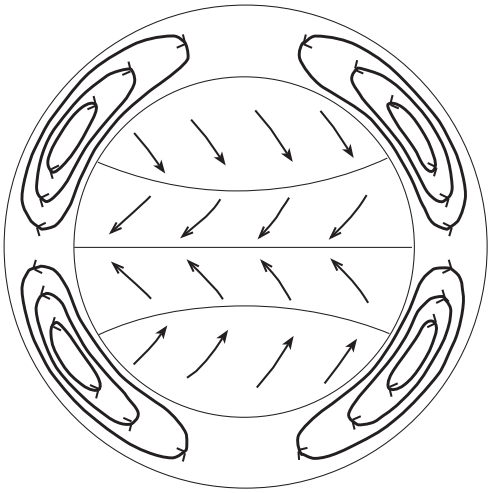

and the formation of storms, can be simulated well for a planet entirely covered by water without any mountains, coasts and vegetation (see Section 1.3). The global-scale features of the climate are modified by the continental distribution and the presence of the largest mountainous ranges, such as the Himalaya, the Andes, the Rocky Mountains, Antarctica, and Greenland. Since these factors are of planetary scale, their impact can be described by standard "low-resolution" general circulation models.

After the planetary scale state of the atmosphere is set, the regional and local climates emerge as the result of an interplay between the planetary climatic state and the local features. This point is illustrated in Section 1.4 with two examples: one about rainfall in Romania and a second one about high sea states in the North Atlantic.

The statement that *the global climate would not be the sum of all regional climates* does not imply that the regional scale dynamics is inconsequential for the global scales. Many processes, such as convection in the atmosphere and in the ocean, play a crucial role in the formation of the global scale state. These processes usually cannot be resolved by the climate models because they take place on scales much too small for such models. However, the details in space and time of these processes are not of importance but only their overall impact. The limited importance of regionally limited changes of the boundary conditions is demonstrated by a numerical experiment on the

effect of the transformation of the North American prairies into crop- and farmland (Section 1.5). The concept of parameterizations of sub-grid scale processes is outlined, and the idea of a randomized design is sketched and motivated.

1.2 The Global View: Energy Balance Models

The simplest conceptual model for the earth's climate, or any other planet's climate is the based on the conservation of energy: In order to have a stationary climate, the time-mean incoming radiation (energy) must be balanced by the same amount of energy radiated back to space. Or, formally:

$$R_{\text{incoming}} = R_{\text{outgoing}} \tag{1.1}$$

Models based on this ansatz[3] are called *energy balance models*, and can achieve considerable complexity (e.g. Crowley and North, 1991).

The sun, being the source of energy in this system, radiates mostly in the short wave band of the spectrum. Part of this incoming radiation is reflected back to space, but another part is absorbed by the earth system, and eventually re-radiated. Since the earth is a relatively cool body, this radiation takes place in the long wave spectral band. Then, the balance (1.1) reads:

$$R_{sw} = \alpha R_{sw} + R_{lw} \tag{1.2}$$

with the *albedo* α and the short wave and long wave radiations R_{sw} and R_{lw}. The incoming short-wave radiation is $R_{sw} = 342\ Wm^{-2}$. The long-wave radiation is a function of the temperature of the radiating body (obeying the Stefan-Boltzmann law)

$$R_{lw} = \kappa\sigma T^4 \tag{1.3}$$

with $\sigma = 5.67 \cdot 10^{-8} Wm^{-2}K^{-4}$ representing a universal constant and κ describing the transmissivity of the earth atmosphere with respect to long-wave radiation (the amount of long-wave radiation emitted at the earth surface which escapes to space). If the system is in equilibrium, we find as temperature for the radiating earth:

$$T_{eq} = \left[\frac{(1-\alpha)R_{sw}}{\kappa\sigma}\right]^{\frac{1}{4}} \tag{1.4}$$

[3] This technical term of German origin is well known among physicists and mathematicians but not entirely so in the meteorological and oceanographic community. "To make an ansatz" means to assume a certain plausible relationship (in this case, equation (1.1)), and to examine if this relationship can be detailed so that it explains certain observed or theoretical "facts".

Figure 1.3: Energy balance diagram. Units of Wm^{-2}. From von Storch (1997).

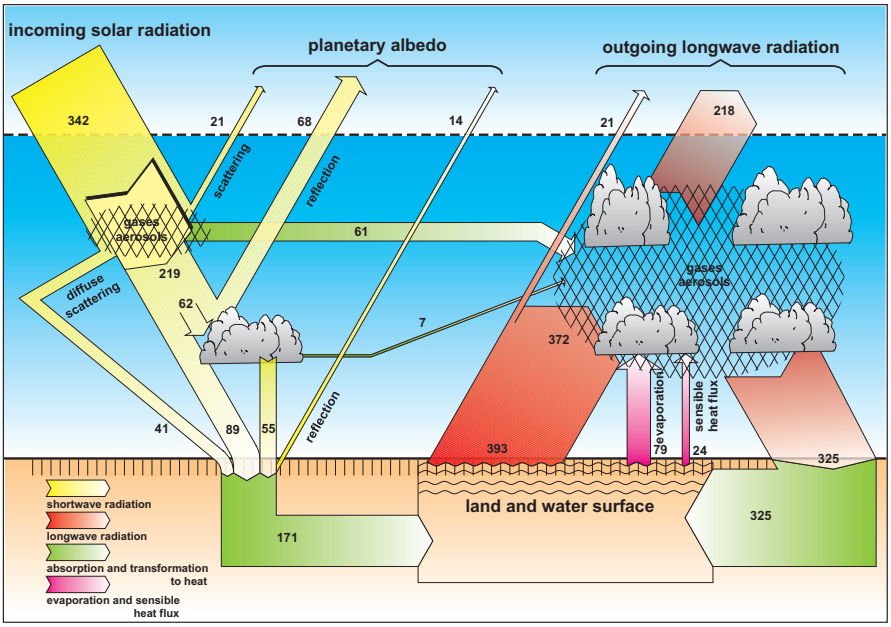

If there were no atmosphere, κ would be unity, and the albedo would be about 15%, so that the resulting equilibrium temperature would be about -4°C. The presence of the atmosphere leads to an increased albedo (clouds) of about $\alpha = 0.30$ but also to a reduced transmissivity of $\kappa = 0.64$. The resulting equilibrium temperature is about 15° C, being close to the observed value.[4]

Figure 1.3 summarizes the globally averaged energy balance. It shows the incoming short wave and outgoing long wave radiative terms as well as the various complications introduced by the presence of gases and particles in the atmosphere which absorb and re-emit radiation. Also some of the energy is absorbed by the surface and released as latent and sensible heat which eventually is radiatively exported from the system at higher levels, in part after condensation. All these processes are hidden in the number κ – or, in other words, these processes are *parameterized* by adding the tuning constant κ in the Stefan-Boltzmann radiation law.

The dynamics of the system may be made more "interesting", by incorporating a nonlinear term, describing the dependency of the albedo on

[4]The similarity of the modeled temperature and the real global mean near-surface temperature does not provide validation of the estimated value of $\alpha = 0.3$; the parameter κ has been chosen so that meaningful numbers emerge - however the choice of κ is fully consistent with physical reasoning about the involved processes.

Figure 1.4: Assumed nonlinear dependency of albedo α upon the global mean temperature. From von Storch (1997)

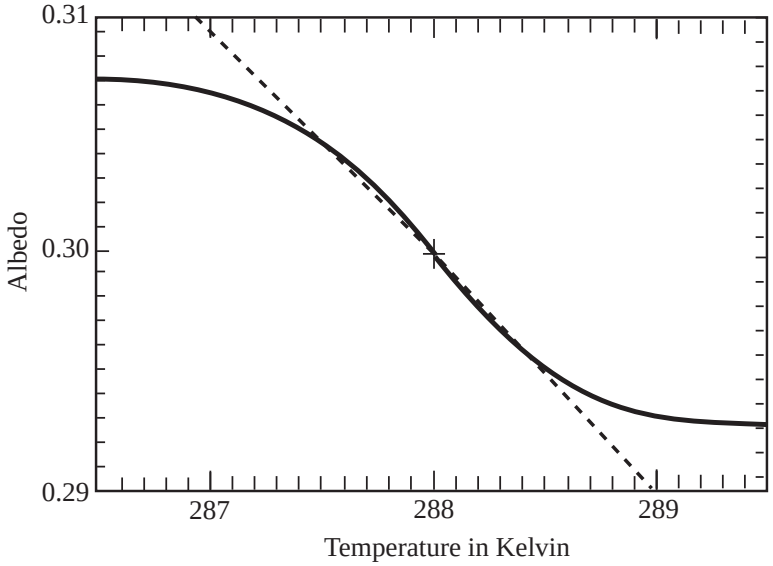

the presence of snow and ice. If more of the earth surface is covered by snow and ice, then the albedo is enhanced and the surface of the earth is colder, and vice versa. An ad-hoc ansatz for this dependency is displayed in Figure 1.4. The intersections with the dashed lines are the three solutions $T_{eq} \approx 287.5K, 288.5K$ and $288K$ of equation (1.4). The first two are stable solutions, i.e, if the system is moved away from the stable solution it returns to it within a characteristic time. The middle solution is unstable, so that any miniscule disturbance will drive the temperature to the nearest equilibrium stable solution temperature. The behavior is described in Figure 1.5.

Further complication can be introduced by noise (see Section 1.5.2) and latitudinal and vertical structures (Crowley and North, 1991). However, all these models have in common that they do not model the *circulation* of the atmosphere. Obviously the circulation is a significant climatic feature, which, among others, causes our daily experience of weather.

1.3 The Global Atmospheric Circulation: Emergence from a State at Rest

In the previous section we have dealt with the climate system as a thermodynamic system which continuously receives energy and re-emits this energy

Figure 1.5: Convergence towards stable equilibrium solution of the Energy Balance Model (1.4) with temperature dependent albedo. From von Storch (1997)

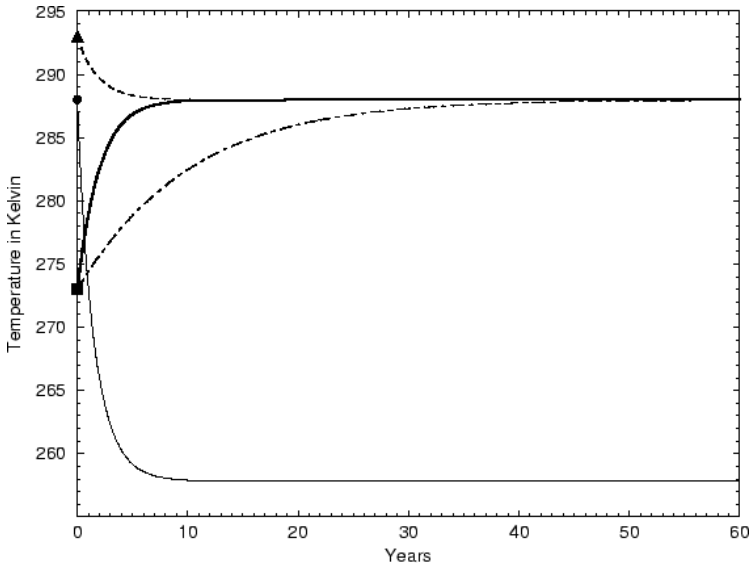

to space. In fact, the thermodynamic system "climate" may be seen as a thermodynamic machine which transforms thermal energy into mechanical energy – in the form of winds in the atmosphere and currents in the ocean. Eventually, the mechanical energy is dissipated to thermal energy which is radiated to space. In this section we will demonstrate what kind of motions our machinery performs – and we will see again that the regional details are insignificant for the planetary scale patterns of the circulation.

Washington (1968) [5] and later Fischer et al. (1991) have performed interesting *numerical experiments* with a *General Circulation Model* (GCM) of the atmosphere (for the design of such models, refer to Washington's contribution to this book in Chapter 2). They both initialized their multi-month simulation of the atmospheric circulation from a state at rest. Washington used realistic topography, land-sea distribution and winter sea surface temperature (SST) distribution, whereas Fischer et al. (1991) used an *aqua planet*, i.e., a planet entirely covered by water with zonally symmetric SST distribution. In both simulations, a realistic planetary scale circulation emerged within one month, or so.

Figure 1.6 displays the evolution of the air-pressure in Washington's ex-

[5] A summary of the experiment is given in the monograph by Washington and Parkinson, 1986, page 209-210.

Figure 1.6: Emergence of the general circulation of the troposphere from an isothermal atmospheric state at rest with a realistic land-sea distribution. The variable shown is the air-pressure. From Washington (1968).

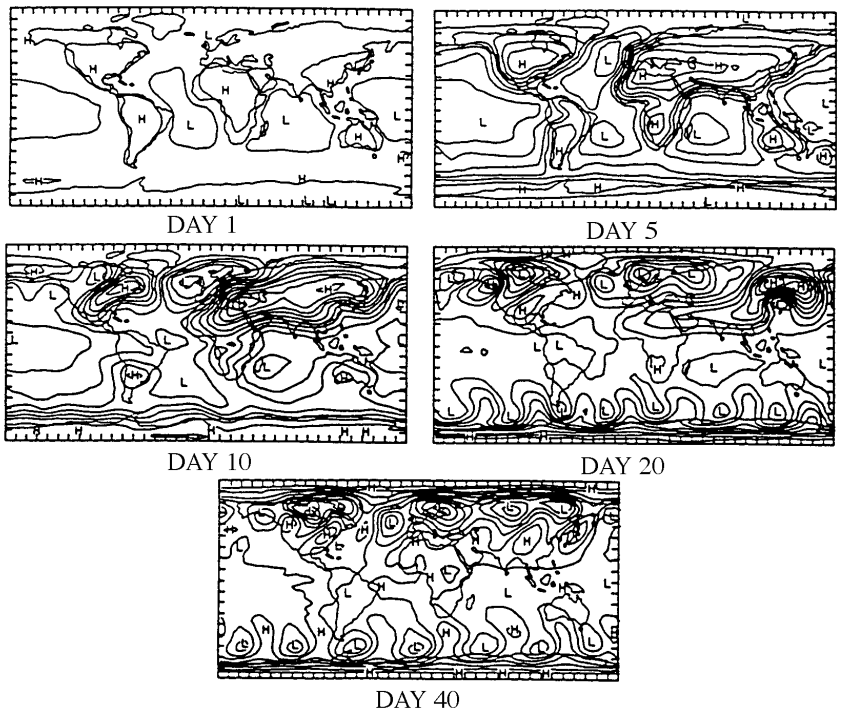

periment - the pressure is falling over the warmer sea and rising over land. However, after about 10 days the system becomes unstable at mid latitudes and weather systems (storms) begin to emerge. After about 40 days, the characteristic macro-turbulent behavior, in particular on the Southern hemisphere, has emerged in the mid latitudes while in the tropics weak pressure gradients prevail.

In Fischer's experiment the initial fingerprint of the land-sea distribution on air pressure does not appear – as there are no continents – and during the first 10 days the atmosphere stays mostly motionless (apart of small meridional winds close to the equator; Figure 1.7b), and almost all transports of heat taken up by the atmosphere at the ocean surface (which represents the input of the short term incoming radiation) takes place by diffusive mechanisms. At about day 10 an almost explosive change takes places in the tropics and wanders in a couple of weeks across the mid and polar latitudes. First, the tropical cells and the trade wind system are built within a couple of days.

Figure 1.7: Emergence of the general circulation of the troposphere from an isothermal state at rest on an aqua-planet. From Fischer et al. (1991). All variables are shown as zonal averages.
a) zonal wind at 950 hPa
b) meridional wind at 950 hPa
c) kinetic energy of the disturbances (i.e. deviations from the zonally averaged state.

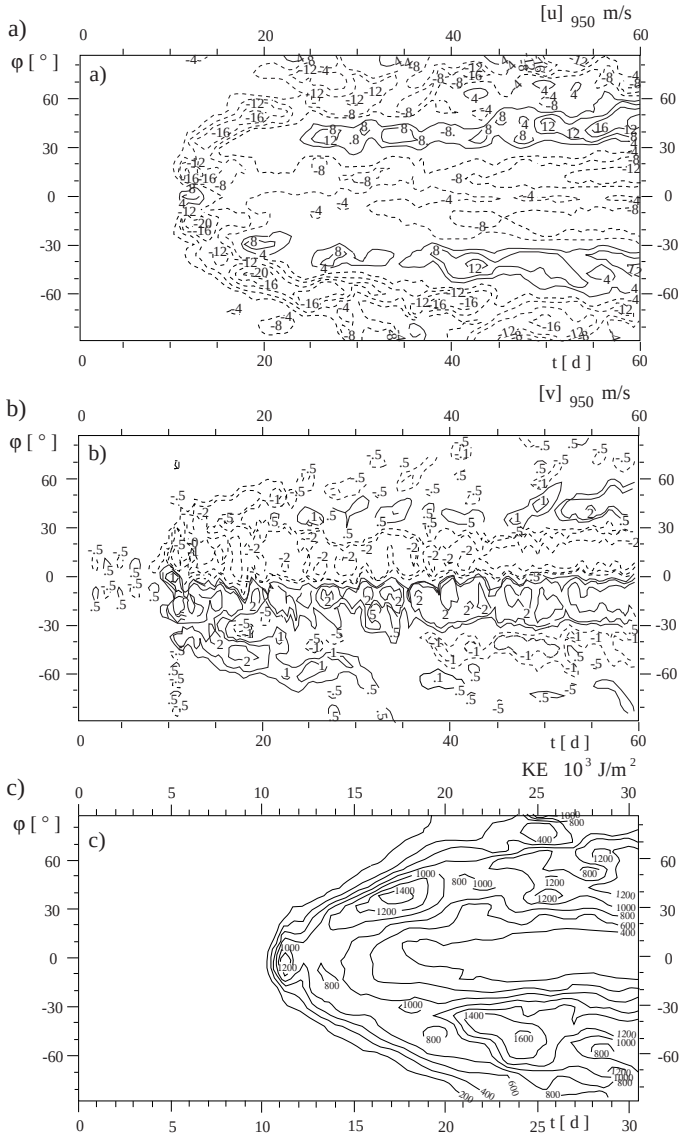

Figure 1.8: Sketch of the general circulation of the atmosphere. Note that the mid latitudes are characterized by unsteady (but statistically quasi-stationary) states with short term baroclinic disturbances. From von Storch et al. (1999).

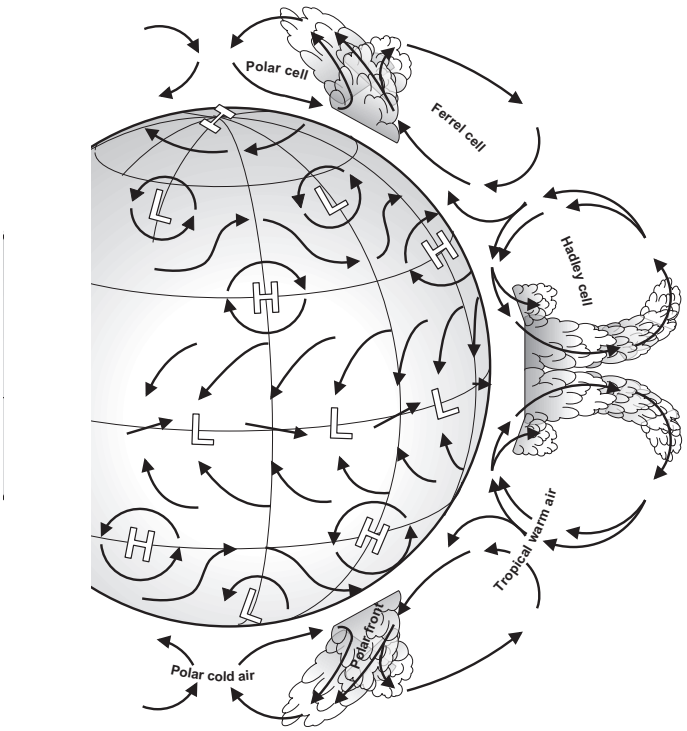

Then, about 20 days after initializing the indirect Ferrell cell with westerly and northerly near-surface winds appear (Figure 1.7a,b) and very vaguely a polar cell. Turbulent motions, as revealed by the energy of disturbances (Figure 1.7c), first show up in the vicinity of the equator, but "drift" within about 10 days to its observed location at mid latitudes.

The eventual state reached within one to two month is in both, Washington's and Fischer's case, very similar to the observed state (as sketched in Figure 1.8). Thus, the pattern of the "planetary scale atmospheric circulation" is unrelated to regional details such as topography or land use. The main elements, such as the lowered geopotential height in polar areas and the lifted height in tropical areas with southwesterly flows across the mid latitude oceans, with elongated mid-latitude jet streams near the tropopause and enhanced baroclinic activities at the exit of the jet-streams (Figure 1.9) are conditioned by planetary scale forcing factors such as global radiation

Figure 1.9: Northern hemisphere long-term mean distributions of geopotential height at 500 hPa. From Risbey and Stone (1996).

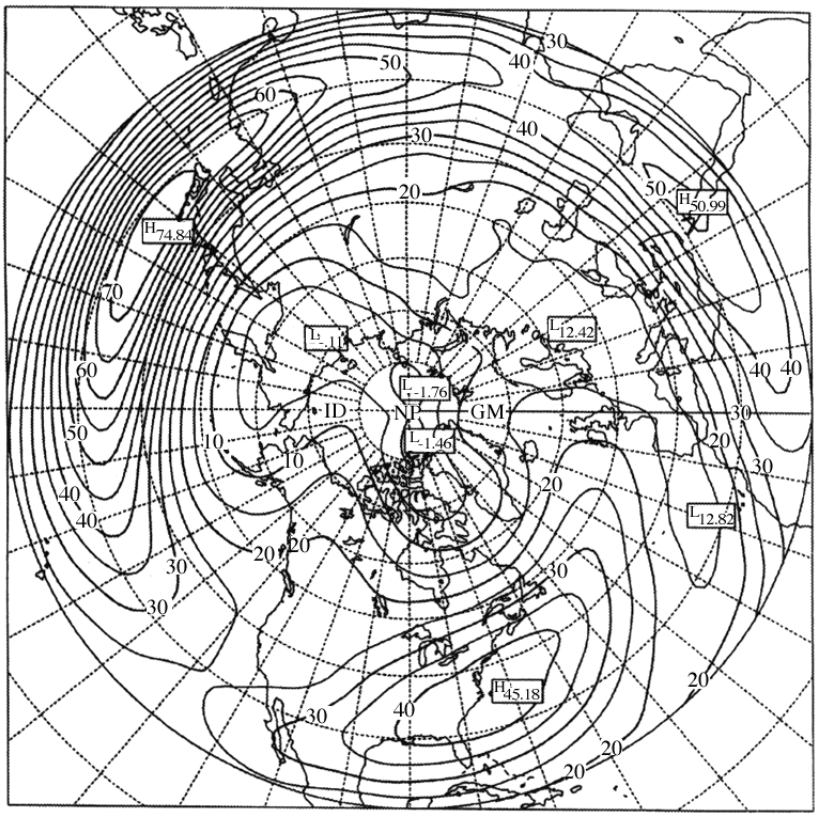

and the planetary scale topography.

1.4 The Regional Climate: Controlled by Planetary Scales

After the planetary scale features of the atmospheric circulation (tropical cells, jet streams, baroclinic zones) are established, these features interact with regional features, such as secondary mountain ranges, coast lines, inland waters. These interactions lead to modifications of the planetary climate on the regional scales - the regional climates. For example, secondary storm tracks may form, for instance in the lee of the Alps over the warm waters of the Mediterranean Sea (both the Alps and the Mediterranean are insignificant features for the formation of the planetary scale climate). Maritime storms

Figure 1.10: Northern hemisphere long-term mean distributions of zonal wind. Other explanations s. Figure 1.9

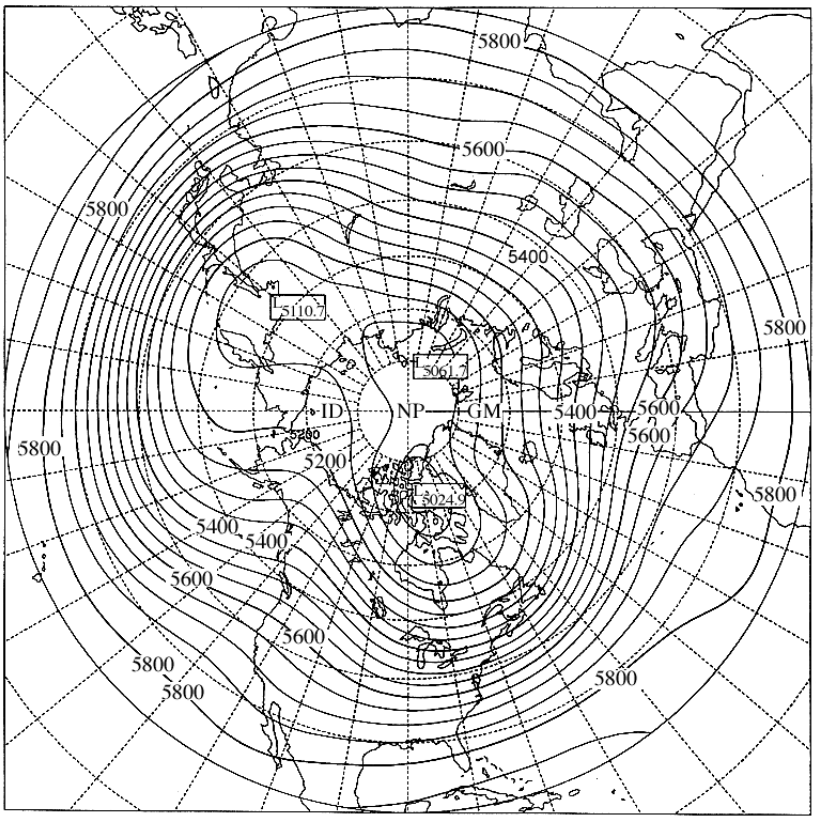

dump abundant rainfall on coastal areas, and the like.

As a demonstration, we show in Figure 1.12 a *composite analysis* of rainfall in the Sacramento Valley (California, USA). The Northern Hemisphere mean distribution of air pressure (at sea level), of 500 hPa height and zonal wind at 200 hPa averaged over all days with maximum local precipitation were calculated, as well as one day before and after this event. Not surprisingly, rainfall tends to be maximal when on the large-scale a storm travels across the area (day 0), coming from the west (where the storms are formed – day -1). After the precipitation, the storms weakens (day +1). The low pressure system is also visible at the middle of the troposphere at 500 hPa by a trough displaced by several tens of degrees to the east compared to its climatological mean state (not shown), and the jet stream, as visualized by the near-tropopause zonal wind, is elongated far to the east (compare with

Figure 1.11: Northern hemisphere long-term mean distributions of the band-pass filtered variance of 500 hPa geopotential height. The filter is selected to retain variability on time scales related to baroclinic processes, i.e. mostly midlatidude storms. Other explanations s. Figure 1.9

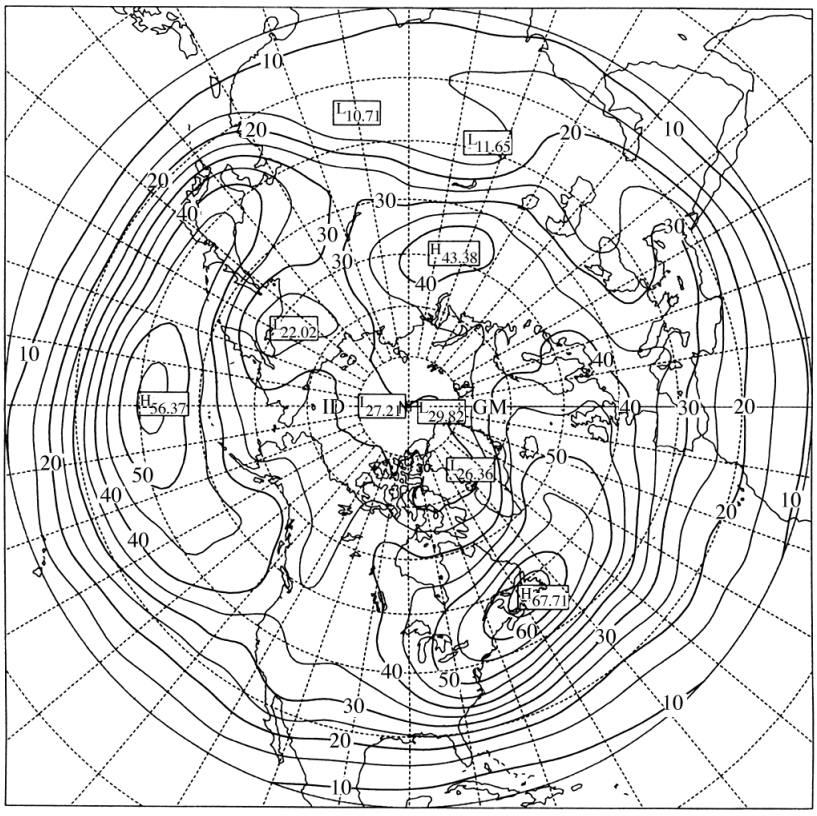

Figure 1.9). Thus, a planetary scale event – the displacement of the trough at 500 hPa and the elongation of the jet stream – eventually lead to a regional event, namely a strong rainfall storm in the Sacramento Valley.

After having illustrated synoptically how the planetary scale variability influences the regional variability, we will demonstrate how the statistics of regional variability, or in another term: the regional climate, is conditioned by the statistics of the planetary scale climate. To do so, we need to formally introduce the concept of conditional statistical models in the following subsection.

Figure 1.12: Composite analysis of air pressure and 200 hPa zonal wind for 10 days with maximum precipitation ("day 0" at a location in the Sacramento Valley (middle) and for the 10 days one day before (top, "day -1") and after (bottom, "day +1") maximum precipitation. From Risbey and Stone (1996).

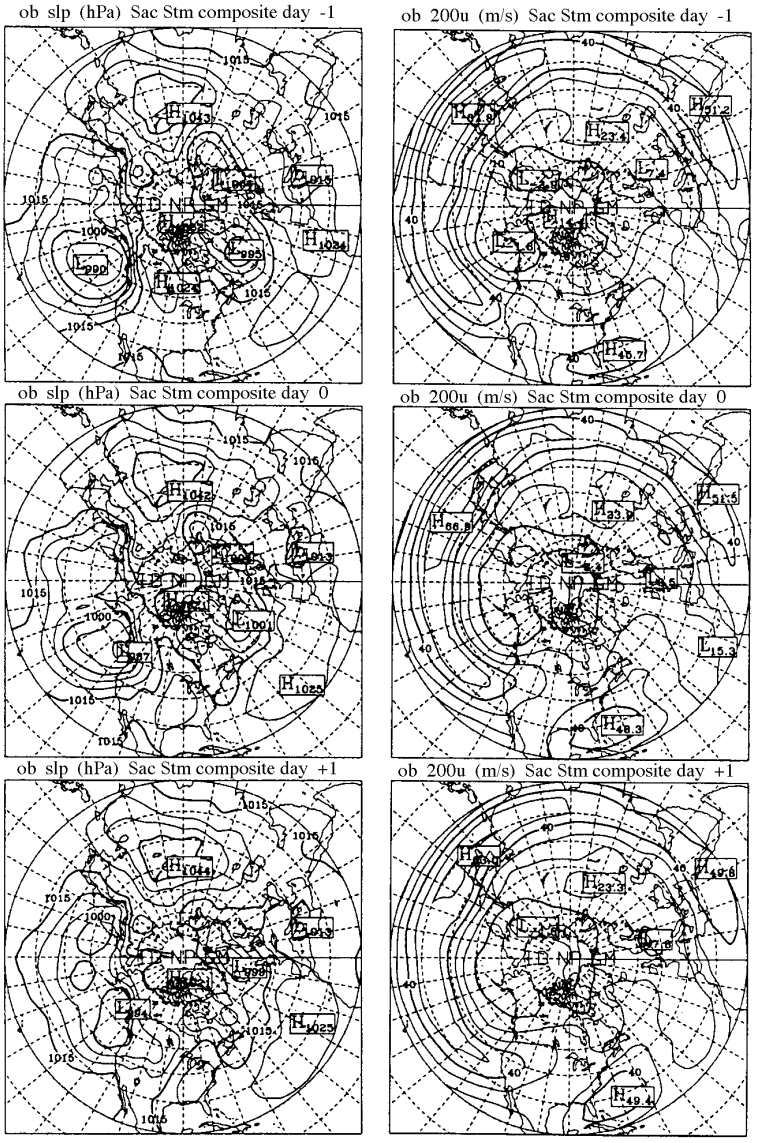

1.4.1 Conditional Statistical Models

If a random variable $\vec{\mathbf{X}}$ is *conditioned* upon another random variable $\vec{\mathbf{G}}$,[6] then the probability density function $F_{\vec{X}}(\vec{x})$ of $\vec{\mathbf{X}}$ may by partitioned such that

$$f_{\vec{X}}(\vec{\mathbf{x}}) = \int f_{\vec{X}|\vec{G}=\vec{g}}(\vec{\mathbf{x}}) f_G(\vec{\mathbf{g}}) d\vec{\mathbf{g}} \tag{1.5}$$

where $f_{\vec{X}|\vec{G}=\vec{g}}(\vec{x})$ is the *conditional* probability function of $\vec{\mathbf{X}}$ provided that the random variable $\vec{\mathbf{G}}$ takes the value $\vec{\mathbf{g}}$, and $f_{\vec{G}}$ is the probability density function of $\vec{\mathbf{G}}$ (cf. Katz and Parlange, 1996).

The expectation and the variance of $\vec{\mathbf{X}}$ may be decomposed:

$$\begin{aligned} \mathrm{E}_X\left(\vec{\mathbf{X}}\right) &= \mathrm{E}_G\left(\mathrm{E}_X\left(\vec{\mathbf{X}}|\vec{\mathbf{G}}\right)\right) & (1.6)\\ \mathrm{VAR}_X\left(\vec{\mathbf{X}}\right) &= \mathrm{E}_G\left(\mathrm{VAR}_X\left(\vec{\mathbf{X}}|\vec{\mathbf{G}}\right)\right) + \mathrm{VAR}_G\left(\mathrm{E}_X\left(\vec{\mathbf{X}}|\vec{\mathbf{G}}\right)\right) & (1.7) \end{aligned}$$

where the subscript indicates with respect to which random variable the operation "expectation" and "variance" is to be executed.

Thus, the overall expected value of $\vec{\mathbf{X}}$ is a weighted mean of the conditional expectations; the overall variance is seen to be attributable to two different sources, namely the mean uncertainty of the conditional distributions, and the variability of the different conditional means.

For further demonstration of this effect, let us consider the regression case. To do so, we assume that the univariate variable $\mathbf{X}$ is normally distributed with mean μ and variance σ_x^2: $\mathbf{X} \sim \mathcal{N}(\mu, \sigma_x^2)$. Let us further assume that the mean state μ depends linearly on a large scale time-dependent state $\mathbf{G}_t$:

$$\mu = \mu_0 + \beta\mathbf{G} \tag{1.8}$$

and that the variability around μ is independent of $\mathbf{G}$. Then

$$\mathbf{X}_t = \mu_0 + \beta\mathbf{G}_t + \mathbf{N}_t \tag{1.9}$$

with a normally distributed variable $\mathbf{N} \sim \mathcal{N}(0, \sigma_n^2)$. If the "driving" process $\mathbf{G} \sim \mathcal{N}(0, \sigma_g^2)$, then

$$\begin{aligned} \mathrm{E}(\mathbf{X}) &= \mu_0 \\ \mathrm{E}(\mathbf{X}|\mathbf{G}_t) &= \mu_0 + \beta\mathbf{G}_t \\ \mathrm{VAR}(\mathbf{X}) &= \mathrm{E}\big((\mathbf{X}-\mu_0)^2\big) = \mathrm{E}\big((\beta\mathbf{G}_t + \mathbf{N}_t)^2\big) = \beta^2\sigma_g^2 + \sigma_n^2 & (1.10)\\ \mathrm{VAR}(\mathbf{X}|\mathbf{G}_t) &= \mathrm{E}\big((\mathbf{X}-\mu_0-\beta\mathbf{G}_t)^2\big) = \sigma_n^2 \end{aligned}$$

This decomposition is a special version of equation (1.7) and attributes part of the $\mathbf{X}$-variance to the internal variability (σ_n^2) unrelated to the driving

[6] For an overview about statistical analysis in climate research, refer to von Storch and Navarra (1995) and von Storch and Zwiers (1998).

process, and the remaining variance to the variability of the driving process itself (σ_g^2).

If we describe the regional climate $\vec{\mathbf{X}}_t$ as the outcome of a stochastic process[7], i.e., when we formally write

$$\vec{\mathbf{X}}_t \sim \mathcal{P}(\vec{\alpha}) \tag{1.11}$$

with a vector of parameters $\vec{\alpha} = (\alpha_1 \dots \alpha_K)$. The probability distribution $\mathcal{P}$ has to be chosen from a suitable family of distribution. In many cases $\mathcal{P}$ will be Gaussian so that $\alpha_1 = \vec{\mu}$ and $\alpha_2 = \mathbf{\Sigma}$, with $\vec{\mu}$ representing the mean vector and $\mathbf{\Sigma}$ the variance-covariance matrix. In other cases, $\mathcal{P}$ may be of considerably more complex form, for instance in case of daily amounts of rainfall (cf. Lettenmaier (1995) or Katz and Parlange (1996)).

Following our previous reasoning, that the regional climate is determined by the planetary scales, we may consider the random process $\vec{\mathbf{X}}_t$ being *conditioned* by the planetary scale variable $\mathbf{G}_t$, or:

$$\vec{\alpha} = \mathcal{F}(G_t) \tag{1.12}$$

so that equation (1.11) is replaced by

$$\vec{\mathbf{X}}_t \sim \mathcal{P}(\mathcal{F}(G_t)) \tag{1.13}$$

In the special case of the regression (1.10), the variability of the regional climate variable is caused by the local uncertainty unrelated to the large-scale dynamics, and to the effect of the large-scale variability.

Different techniques may be used to actually estimate the conditioning relationship (1.13) from observational data. The classical approach of synoptic climatology is to determine *Großwetterlagen*, i.e. a finite number of typical weather situations, and to determine for each of these Großwetterlagen the regional weather, which can be done empirically (Bárdossy and Plate, 1992; Conway et al., 1996; Enke and Spekat, 1997) or with dynamical models (Frey-Buness, 1995; Fuentes and Heimann, 1996). Nonlinear techniques refer to neural networks (Hewitson and Crane, 1992, 1996), classification and regression trees or analog specifications (Zorita et al., 1995).

A widely used technique is (linear) regression, which is often combined with linear filter techniques (von Storch et al., 1993; Kaas et al., 1996). A typical representative of this class is *Canonical Correlation Analysis* (CCA; von Storch and Zwiers, 1998), which identifies in the paired vectors $(\vec{\mathbf{G}}_t, \vec{\mathbf{X}}_t)$

[7]This is done explicitly by hydrologists when they build weather generators, see for instance Lettenmaier (1995).

vectors $\vec{p}_j^G$ and $\vec{p}_j^X$ so that

$$\vec{\mathbf{G}}_t = \sum_{j=1}^{J} g^j(t)\vec{p}_j^G \tag{1.14}$$

$$\vec{\mathbf{X}}_t = \sum_{j=1}^{J} x^j(t)\vec{p}_j^X \tag{1.15}$$

The coefficients $g^j(t)$ and $x^j(t)$ with different indices are pairwise uncorrelated, and coefficients with identical indices share maximum correlations ρ_j. Then, the regression model is

$$\mathrm{E}\left(\vec{\mathbf{X}}_t|\vec{\mathbf{G}}_t\right) = \sum_{j=1}^{J} \rho_j g^j(t)\vec{p}_j^X \tag{1.16}$$

Usually, the number J of retained terms in (1.14,1.15) is small, so that the truncated expansions (1.14,1.15) represent efficient filtering operations. Note that Canonical Correlation Analysis is intrinsically symmetric, and puts the same weight on the "predictor" $\vec{\mathbf{G}}_t$ and on the "predictand" $\vec{\mathbf{X}}_t$.

Another technique, so far hardly used to this end, is *Redundancy Analysis* (RDA; Tyler, 1982; von Storch and Zwiers, 1998). In this case, also expansions like (1.14,1.15) are determined, but the predictor and predictand are treated differently. For any set of linearly independent patterns $\{\vec{p}_j^G; j = 1 \ldots J\}$ there is a uniquely determined regression operator $\mathcal{R}_J$ on $\vec{\mathbf{X}}_t$ so that

$$\hat{\vec{\mathbf{X}}}_{t,J} = \mathcal{R}_J \sum_{j=1}^{J} g^j(t)\vec{p}_j^X \tag{1.17}$$

represent a maximum of variance of $\vec{\mathbf{X}}_t$. The redundancy pattern set $\{\vec{p}_j^G, j = 1 \ldots J\}$ is defined to be that set with minimum $\textsc{Var}\left(\vec{\mathbf{X}}_t - \hat{\vec{\mathbf{X}}}_{t,J}\right)$. Then, an orthonormal set of vectors $\{\vec{p}_j^X; j = 1 \ldots J\}$ may be determined so that the regression $\mathcal{R}_J$ maps the predictor patterns $\vec{p}_j^G$ on the predictand patterns $\vec{p}_j^X$. After these manipulations, equation (1.16) may be written as (1.17).

In both cases, CCA and RDA, the resulting patterns may be interpreted such that the emergence of the predictor pattern $\vec{p}_j^G$ on the planetary scale atmospheric state coincides with the emergence of the predictand pattern $\vec{p}_j^X$ on the regional scale state. The difference between the two techniques is that CCA maximizes the correlation of the link whereas RDA maximizes the amount of variance of the regional scale variable describable by the planetary scale variable. In the examples considered so far, the patterns identified by CCA and RDA were rather similar, with slightly larger correlation coefficients in case of CCA and somewhat larger proportions of variances of the predictand described by the predictor in case of the RDA.

In the following applications of CCA and RDA are demonstrated.

Figure 1.13: The patterns of the first canonical pair of the winter mean SLP (top; contour 0.2 mb; the area of Romania is encircled by a heavy line) and total winter Rumanian precipitation (bottom; contour 20 mm; the Carpathian mountain range as well as the Black Sea area is marked by stippling). Continuous lines mark positive values, and dashed lines negative values. From Busuioc and von Storch (1996).

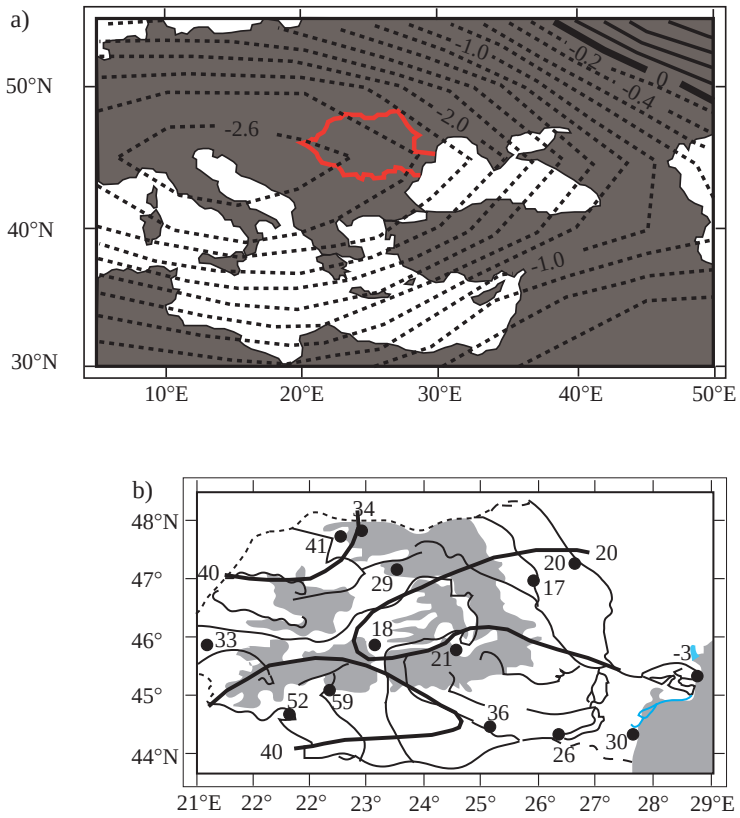

1.4.2 The Case of Rumanian Precipitation

In several studies, the control of regional precipitation by the large scale flow has been studied and demonstrated. In the following we describe results obtained for Romania (Busuioc and von Storch, 1996). The predictand variable is winter mean precipitation amount at 14 stations and the predictor variable is chosen to be the winter mean air pressure distribution (SLP) in $30-55°N$ and $5-50°E$. The data used in this study, from 1901-88, may be considered reasonably homogeneous.[8]

[8] Air pressure is often used in this type of "downscaling" studies (cf. von Storch et al., 1993; Hewitson and Crane, 1996). This pressure data set (Trenberth and Paolino, 1980)

Figure 1.14: The patterns of the second canonical pair of the winter mean SLP (contour 0.2 mb) and total winter Rumanian precipitation (contour 20 mm). Continuous lines mark positive values, and dashed lines negative values. From Busuioc and von Storch (1996).

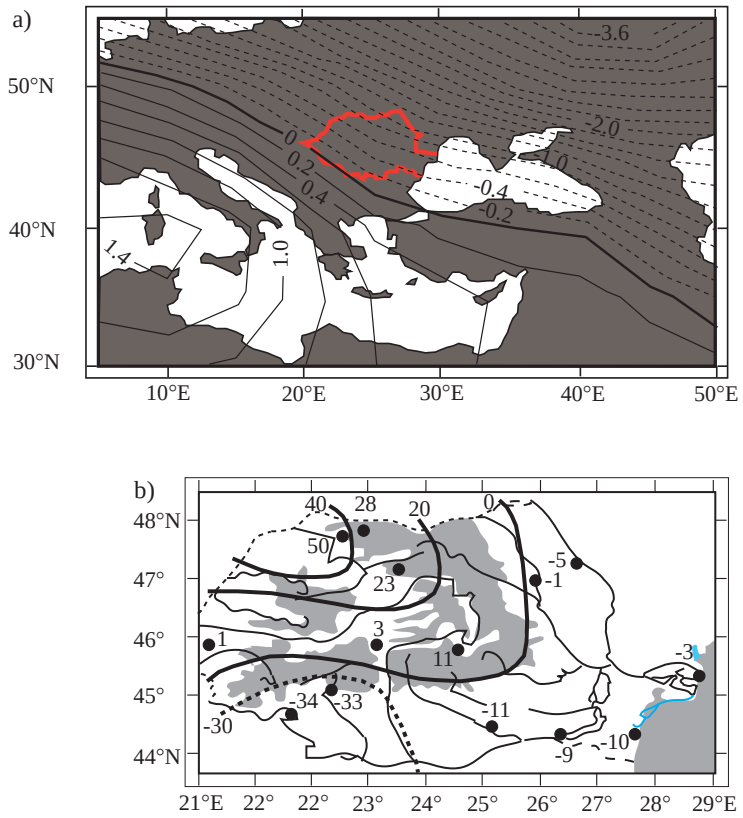

The first CCA pair exhibits a correlation between the precipitation and SLP coefficient time series of 0.84. They explain 35% of the total seasonal mean SLP variance and 47% of the total precipitation variance. The patterns (Figure 1.13) represent a link that is reasonable from the physical point of view: Low pressure over Europe and the Mediterranean basin guides maritime air and precipitating weather systems into Romania, such that above normal precipitation is recorded. The maximum values of almost 59 mm are

---

does not represent "observed" data but represents an analysis of instrumental data. Apart from near surface temperature, this pressure data set is the only one for which a century long observational record with planetary scale coverage and few inhomogeneity problems exist.

Figure 1.15: Normalized time components of the first (a) and second (b) CCA patterns of SLP anomalies (continuous line) and Rumanian precipitation anomalies (dashed line). The vertical arrows mark change points in both coefficient time series. From Busuioc and von Storch (1996).

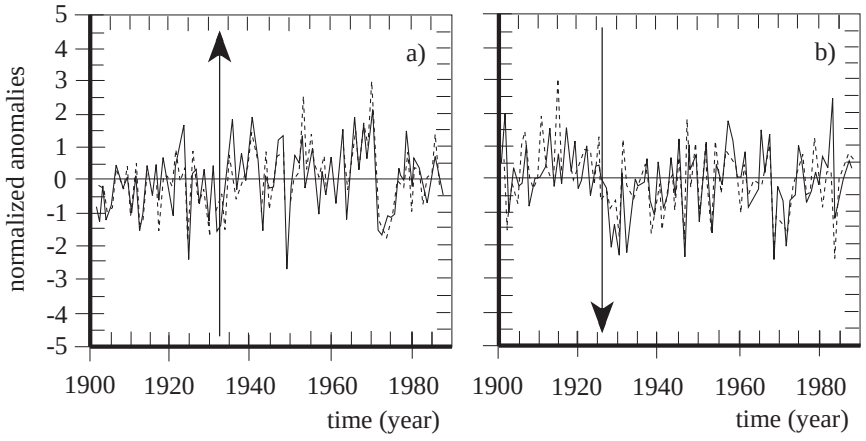

in the southwest and the minimum values of 17 mm in the northeast that shows the orographic perturbation effect of the Carpathian mountains.[9]

The second CCA (0.65 correlation) explains 31% of the total SLP variance and 20% of the total precipitation variance. The patterns (Figure 1.14) suggest another physically plausible link: The SLP pattern describes a northwesterly flow that affects mostly the intra-Carpathian region where the positive precipitation anomalies are emphasized, the highest (of almost 50 mm) being in the northwest.

In Figure 1.15a the time coefficients of the first CCA pair are shown. The year-to-year variations are coherent. An inspection with the Pettitt-test of both time coefficient time series reveals for both, independently, the presence of an upward change-point, i.e., a displacement of the time mean, at about 1933. This finding suggests that the change point detectable in the precipitation series, is not due to an inhomogeneity[10] but is a real feature; in fact *this systematic change in precipitation may be traced back to a change of the large-scale circulation.*

[9]Note that the sign of the two patterns is arbitrary. If both patterns are sign-reversed, the same link is described - high pressure over Europe guide continental air into Romania, and there the precipitation is reduced by 17 to 59 mm.

[10]For problems with observational records due to changes in the instrumentation, observational practices, displacements of the instruments and other reasons, refer to, for instance, Karl et al. (1993) or Jones (1995).

A second downward change-point at about 1969 is signaled by the Pettitt statistic[11] when the time interval is limited to 1935 – 1988. This second change point is again consistent with the analysis of the individual precipitation time series (not shown).

Figure 1.15b shows the time coefficients of the second CCA pair. The year-to year variations are fairly coherent. Both curves share a simultaneous downward change-point in the mid 1920's.

The results presented so far support the notion that Rumanian winter precipitation statistics are to large extent determined by the large-scale European SLP distribution.

1.4.3 The Case of Short Term Event Statistics

The background of this example is the following: Data about wave height (sea state) are available from reports about visual assessments from ships of opportunity and lighthouses, from wave rider buoys and ship borne wave riders at ocean wather stations; also wave heights maps have been constructed for the purpose of ship routing from wind analyses (WASA, 1998). These data are sparse, and suffer from inhomogeneities of various kinds, or their records are too short for allowing an assessment about changes in the past century.

Thus, using observational data alone is hardly sufficient for getting information about interdecadal variability of wave statistics. An option for overcoming this problem is a combined statistical/dynamical reconstruction which makes use of a "hind-cast" simulation with a dynamical wave model, forced with observed wind fields over a limited time for which the wind data are believed to be of sufficient quality and little affected by improving analysis routines.[12]

As a second step, the wave heights, derived from the hind-cast simulation, are considered as "quasi-observations" and are used for building a statistical model, linking the wave height data at one location to a variable which has been monitored for more than a century, namely mean air pressure distribution. In the last step, the constructed statistical model is fed with the observed air pressure from the beginning of the century onward, and a plausible estimate of wave height statistics for the entire century is obtained. In the following we present the statistical model.

In this case we bring together "apples" and "oranges", i.e. two vector quantities which are note directly linked together. One vector time series, $\vec{\mathbf{S}}_t$,

[11] An objective technique for the identification of change points was introduced by Pettitt (1979); for a critique, see Busuioc and von Storch (1996).

[12] Note that the question of whether weather maps, and their surface winds, are homogeneous or introduce artificial signals, such as increasing frequencies of extreme events, into the hind-cast, is a problem difficult to assess - and a possibility which can not be ruled out in general.
Improving analyses procedures, be it because of more or better observations or because of more intelligently designed dynamical and statistical analysis tools, lead to the emergence of more details in weather maps and, therefore, larger extremes.

Table 1.1: Characteristic anomalies of intra-monthly percentiles of significant wave height at the oil field "Brent" ($61°N$, $1.5°E$) northeast of Scotland in winter (DJF) as obtained in a Redundancy Analysis.
The j-row is the j-th redundancy vector $\vec{p}_j^X$. This vector accounts for ϵ_j of the variance of $\vec{\mathbf{X}}$.

	wave height			
$\kappa =$	50%	80%	90%	ϵ_j
j		[cm]		[%]
1	-81	-107	-114	94
2	-32	-2	25	5

Table 1.2: Correlation between hind-casted and reconstructed quantile time series, and proportion of described variance of wave height at "Brent" (see Figure 1.16).

	wave height			
quantile	50%	80%	90%	units
correlation	83	82	77	%
described variance	70	66	60	%

represents the winter (DJF) monthly mean air-pressure distributions in the North Atlantic. The other vector time series, $\vec{\mathbf{X}}_t$, is formed by the 50%, 80% and 90% quantiles of the *intra-monthly distributions* of significant wave height at the oil field *Brent* (approximately $61°N, 1.5°E$; northeast of Scotland)

$$\vec{\mathbf{X}}_t = \begin{pmatrix} q_{50\%} \\ q_{80\%} \\ q_{90\%} \end{pmatrix}_t \tag{1.18}$$

Both vector time series are centered, so that the air pressure values and percentiles are deviations from their long-term mean.[13]

The *monthly mean* of North Atlantic SLP is only indirectly linked to the *intra-monthly percentiles*: the storms affect both, the monthly mean air pressure distribution as well as the distribution of wave heights within a month at a specific location. Of course, the storm activity may also be seen as being conditioned by the monthly mean state.

The daily wave height data are taken from a hind-cast simulation over 40 years (Günther et al., 1998).[14] A Redundancy Analysis (RDA) of the two vector time series is performed in order to detect the dominant coupled

[13] Therefore the percentiles are no longer ordered and it may happen that $q_{50\%} > q_{90\%}$.

[14] The following analysis is based on the assumption that the hind-cast is describing the real evolution sufficiently well and that modifications in analysis of the driving wind field have no significant effect on the statistics of the hind-cast.

Figure 1.16: First two monthly mean air pressure anomaly distributions identified in a Redundancy Analysis as being most strongly linked to simultaneous variations of intra-monthly quantiles of significant wave height at Brent $(61^\circ N, 1.5^\circ E)$. The anomalies of the quantiles at that position are listed in Table 1.1.

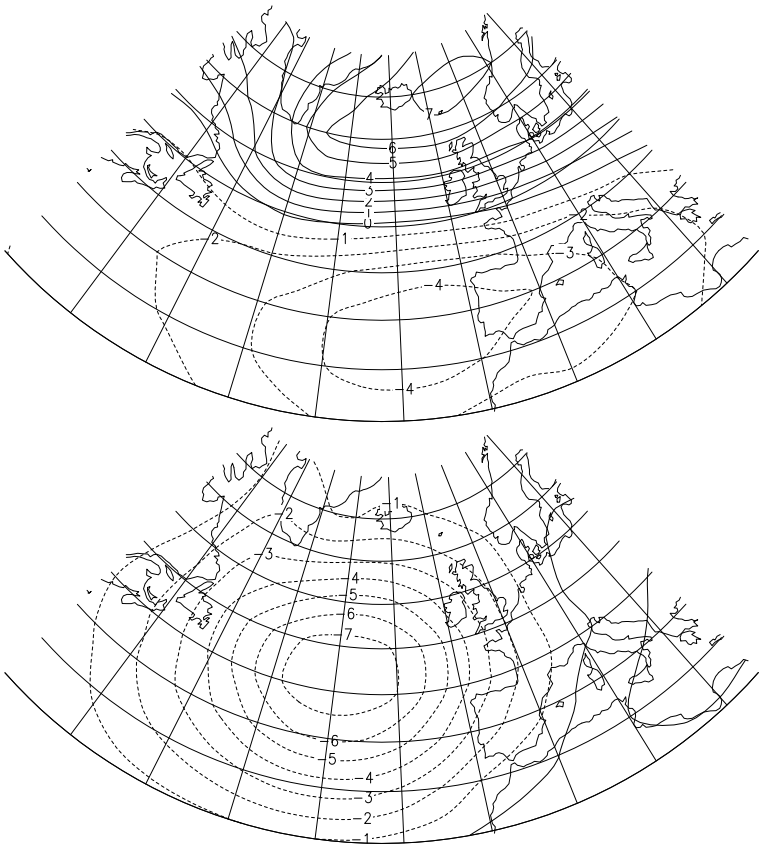

anomaly patterns in the mean air pressure and in the intra monthly wave height percentiles. The SLP patterns $\vec{p}_j^{\,G}$ are shown in Figure 1.16, and the pattern for the intra-monthly percentiles $\vec{p}_j^{\,X}$ are given in Table 1.1 together with the correlations and the proportion of $\vec{\mathbf{X}}$-variance represented by the $\vec{p}_j^{\,X}$-patterns. The RDA coefficients are normalized to unity so that the three components of $\vec{p}_j^{\,X}$ may be interpreted as anomalies which occur typically together with the "field distribution" $\vec{p}_j^{\,G}$.

The first air pressure pattern is closely related to the *North Atlantic Os-*

Figure 1.17: Reconstructed (continuous line) and hind-casted (dashed line; 1955-94) anomalies of 90% quantiles of significant wave heights at "Brent" ($61°N$, $1.5°E$). Units: m.

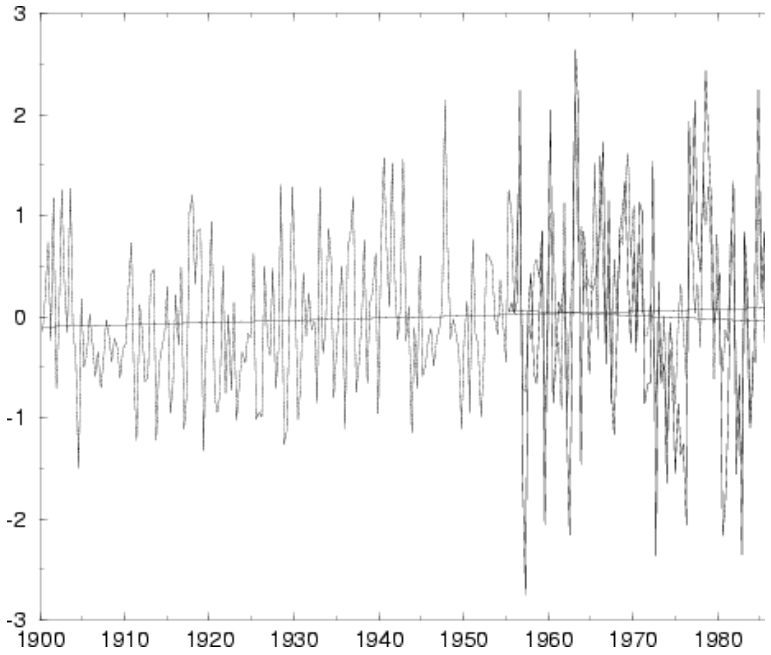

cillation (van Loon and Rogers, 1978). A weakened NAO in the monthly mean is associated with an enhancement of all intra monthly percentiles of significant wave heights. In effect, this pattern describes a shift of the intra-monthly distribution towards smaller waves.

The second pattern describes a mean easterly flow across the northern North Sea; the 50% quantile of the wind sea is reduced by 30 cm, whereas the 90% is enhanced by 30 cm. When this monthly mean air pressure pattern prevails then there is a tendency for the wave height distribution to be widened, while the reversed pattern goes with a narrowed intra monthly distribution of wave heights.

With this regression model (1.17), the observed monthly mean air pressure anomaly fields $\vec{\mathbf{G}}_t$ from 1899 until 1994 were used to estimate the time series of the percentiles of significant wave height at the oil field "Brent". The last 40 years may be compared with the hind-cast data, whereas the first five decades represent our best guess and can not be verified at this time. For 90% quantiles of wind sea height the reconstructed time series 1899-1994 and

the hind-casted time series 1955-94 are displayed in Figure 1.17.

In the past four decades, the correlation between hind-cast and statistically derived heights is good (Table 1.2) As with all regression models, the variance of the estimator is smaller than the variance of the original variable: $\text{VAR}\left(\hat{\vec{\mathbf{X}}}\right) < \text{VAR}\left(\vec{\mathbf{X}}\right)$, which makes sense, as the details of the wave action in a month are not completely determined by the monthly mean air pressure field (see Figure 1.6). Thus, the vector of percentiles is made up of an externally determined component $\hat{\vec{\mathbf{X}}}$ and a component not or only indirectly related to the large-scale state of the atmosphere. To first order approximation, the difference $\vec{\mathbf{X}} - \hat{\vec{\mathbf{X}}}$ may be modeled as white, or maybe red, noise (cf., von Storch, 1997).[15]

1.5 Feedback of Regional Scales on Global Scales

Earlier in this Chapter we have demonstrated the validity of Hadley's approach for understanding climate, namely that the climatic features form in a cascade of decreasing spatial (and temporal) scales. But what about the geographers' Köppen-ansatz, namely that the small scale pieces add to a global entity? Is the global climate conditioned by the regional climates?

The answer is, in principle, positive. First, since the dynamics of the atmosphere are highly non-linear, we may expect each detail to matter for the dynamics – the famous metaphor of the butterfly flapping its wings and by that changing rainfall in Paris (cf. Inaudil et al., 1995). However, we must expand the metaphor and take into account that myriads of butterflies are flapping their wings all the time, and then the question is whether an individual butterfly matters in practical terms.

To give a real-world example: Is there a significant impact if somebody ignites many oil wells in the Kuwait area? As everybody knows, this really happened in 1991 - and before the event the public was greatly concerned about this perspective. Respectable scientists voiced grave concerns that such an event would lead to a situation comparable to the disastrous nuclear winter scenario. The effect was indeed locally disastrous, but the overall effect on the planetary scale turned out to be insignificant (for a photographic account, see Cahalan, 1992; for simulations refer to Bakan et al., 1991; Browning et al., 1991).

Another case refers to a case of an anthropogenic climate change experiment, namely the conversion of the North American prairies into farm land in the last century. Even though no representative observational record from the time before the conversion is available, neither on the regional scale nor on the planetary scale, the case may be studied through a GCM experiment

[15] See also the concept of randomized parameterizations discussed in Section 1.5.2.

Figure 1.18: Number of influences on a spatial scale, originating from smaller and larger scales.
(a) full system.
(b) truncated system.

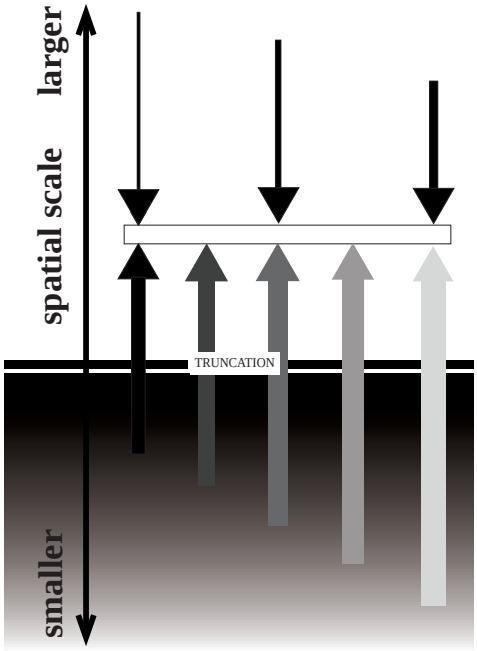

(Copeland et al., 1996). They ran a paired simulation under identical conditions apart of the specified land-use in North America. One simulation was done with present day land-use, and the other with *potential vegetation*. Such a potential vegetation is determined like Köppen's climate map (Figure 1.1), namely though an empirically determined bivariate function, operating with temperature and precipitation, specifying typical vegetation. No planetary scale changes are induced (not shown) only some regional changes mostly in the vicinity of the altered landscape.

On the other hand, local processes, such as the impact of a meteorite or a major eruption of a volcano, such as the Krakatoa eruption in 1883, may have a significant effect on the planetary scale state of the climate – mainly by injecting large amounts of aerosols on a planetary scale into the stratosphere.

If we disregard such dramatic effects, though, the details of regional processes usually are unimportant. Let us discuss this problem in a somewhat

more systematic manner. Let us assume that the climate state is given by a variable Φ and its dynamics by

$$\frac{\partial \Phi}{\partial t} = \mathcal{R}(\Phi) \tag{1.19}$$

with a suitable operator $\mathcal{R}$. We may expand the climate variable into an infinite series

$$\Phi = \sum_k \Phi_k = \sum_k \sum_{j=1}^{k} \phi_{k,j} \tag{1.20}$$

where the $\phi_{k,j}$ may be spherical harmonics or other suitable orthogonal functions. The index k represents the spatial scale L/k with some characteristic length scale L. The index j counts the independent processes with spatial scale L/k. Note that the number of these processes increases with decreasing spatial scale. Thus, the dynamics (1.20) may be expressed for each spatial scale

$$\begin{aligned} \frac{\partial \Phi_k}{\partial t} &= \sum_{j \le k} \mathcal{R}_{k,j}(\Phi_j) + \sum_{j>k} \mathcal{R}_{k;j}(\Phi_j) \\ &= \sum_{j \le k} \sum_{l=1}^{j} \mathcal{R}_{k,j;l}(\phi_{j,l}) + \sum_{j=k+1}^{\infty} \sum_{l=1}^{j} \mathcal{R}_{k,j;l}(\phi_{j,l}) \end{aligned} \tag{1.21}$$

The first sum in the last expression features a finite, and often small number of terms, whereas the second features infinitely many terms (cf. Figure 1.18a). If we assume that processes of comparable scales have similar influences in (1.21), then a specific process (j, l), as represented by $\mathcal{R}_{k,j;l}$ cannot be important for the spatial scale L/k with $k \ll j$, even if the sum over all l may be so.

In General Circulation Models of the atmosphere and of the climate system as a whole, the dynamics cannot be expressed through (1.21), requiring *truncation* of the range of j:

$$\begin{aligned} \frac{\partial \Phi_k}{\partial t} &= \sum_{j \le k} \mathcal{R}_{k,j}(\Phi_j) + \sum_{j=k+1}^{N} \mathcal{R}_{k;j}(\Phi_j) \\ &= \sum_{j \le k} \sum_{l=1}^{j} \mathcal{R}_{k,j;l}(\phi_{j,l}) + \sum_{j=k+1}^{N} \sum_{l=1}^{j} \mathcal{R}_{k,j;l}(\phi_{j,l}) \end{aligned} \tag{1.22}$$

i.e., only processes with a scale of at least L/N are considered, while all processes at scales smaller than L/$N$are discarded - the situation is sketched in Figure 1.18b. The effect of this truncation is worst for scales L/k close to L/N, and least for scales $k \gg N$. However, since the differential equations are non-linear and are integrated forward in time, the errors, which are limited

in the beginning of the integration to the small resolved scales eventually are transported to larger and larger scales and finally ruin the entire simulation (cf, Roeckner and von Storch, 1980). Thus, the disregarded sub-grid scale processes must somehow be brought into the equation (1.22). The technique for doing so is called *parameterization*. The idea of these parameterizations will be explained in the next subsection.

1.5.1 Parameterizations

Let us write a climate variable Φ as a sum of the large-scale resolved component $\bar{\Phi}$ and an unresolved part Φ'

$$\Phi = \bar{\Phi} + \Phi' \tag{1.23}$$

Then, our basic differential equation (1.19) is replaced by

$$\frac{\partial \bar{\Phi}}{\partial t} = \mathcal{R}_{\Delta x}(\Phi) \tag{1.24}$$

with a modified operator $\mathcal{R}_{\Delta x}$ resulting from the full operator $\mathcal{R}$ after introducing a truncated spatial resolution Δx (this could be the global or regional average). In general, this operator may be written as

$$\mathcal{R}_{\Delta x}(\Phi) = \mathcal{R}(\bar{\Phi}) + \mathcal{R}'(\Phi') \tag{1.25}$$

with an operator $\mathcal{R}'$ describing the net effect of the sub grid scale variations represented by Φ'. With this set-up, the system (1.24) is no longer closed and can therefore no longer be integrated. To overcome this problem, conventional approaches assume that the "nuisance" term $\mathcal{R}'(\Phi')$ is either irrelevant, i.e.,

$$\mathcal{R}'(\Phi') = 0 \tag{1.26}$$

or may be *parameterized* by

$$\mathcal{R}'(\Phi') \approx \mathcal{Q}(\bar{\Phi}) \tag{1.27}$$

with some empirically determined or dynamically motivated function $\mathcal{Q}$.

This is the conventional approach which is routinely and massively used not only in all climate models, but also in many other environmental models. Processes which are parameterized in climate models are the turbulence in the planetary boundary layer, mixing of matter, momentum and energy, convection, interaction of radiation with clouds, aerosols and gases, the emission of matter and energy from the surface, the routing of rain water into rivers and many more (cf. Figure 1.3). Papers dealing with the design and the test of the effect of different parameterizations are manifold – examples are Brinkop and Roeckner (1995), Lohmann and Roeckner (1993) or Hense et al. (1982).

In the following subsection a somewhat different concept of parameterizations is introduced, which considers the effect of the unresolved scales as only partially determined by the resolved scales (von Storch, 1997). This concept has not yet been tested and only preliminary examples can be offered.

1.5.2 Randomized Parameterization

While both specifications (1.26,1.27) return an integrable equation (1.24), they both have to assume that the local scale acts as a deterministic slave of the resolved scales. However, as we have seen, in reality there is variability at local scales *unrelated to the resolved scales*. Thus, equation (1.24) should take into account that $\mathcal{R}'(\Phi')$ can not completely be specified as a function of $\bar{\Phi}$, but that formulation (1.27) should be replaced by

$$\mathcal{R}'(\Phi') \sim \mathcal{S}(\vec{\alpha}) \tag{1.28}$$

with a random process $\mathcal{S}$ with parameters $\vec{\alpha}$ which are conditioned upon the resolved state $\bar{\Phi}$:

$$\mathcal{R}'(\Phi') \sim \mathcal{S}(\mathcal{F}(\bar{\Phi})) \tag{1.29}$$

When the mean value μ is the only parameter in the vector $\vec{\alpha}$ which depends on $\bar{\phi}$, then the distribution $\mathcal{S}$ may be written as

$$\mathcal{S}(\mathcal{F}(\bar{\Phi})) = \mu(\bar{\Phi}) + \mathcal{S}' \tag{1.30}$$

with a conditional mean value and a random components with zero mean value ($\mathrm{E}(\mathcal{S}') = 0$) and uncertainty unrelated to the resolved scales. Specification (1.27) equals specification (1.30) if $\mathcal{S}' = 0$ and $\mu(\bar{\Phi}) = \mathcal{Q}(\bar{\Phi})$.

For demonstration of the difference between the two specifications, (1.27) and (1.30), we discuss Figure 1.19 displaying various "measurements" of the drag coefficients c_D of the sea surface sorted according to the value of the la"10 m wind" $|\vec{u}_{10}|$ during neutral conditions (from De Cosmo et al., 1996). In this case we consider the wind measured at a height of 10 m as the "resolved scale" parameter $\bar{\Phi}$, which is representative for a certain spatial and temporal scale and is readily observable. The transfer of momentum $\vec{\tau} = \mathcal{R}(\Phi')$ through the interface of ocean and atmosphere, however, depends on the variance of short-term and smallest scale variations of the wind. The latter quantity can be determined only in expensive observational campaigns, but it has long been known that it can be approximated by the "bulk formula"

$$\vec{\tau} \approx c_D \rho |\vec{u}_{10}| \vec{u}_{10} \tag{1.31}$$

where c_D is considered to depend on the thermal stability and the wind speed. Formula (1.31) represents the classical case of a parameterization, namely the frictional effect of small-scale short-term fluctuations of wind on the atmospheric flow. Figure 1.19 displays a scatter of points, each representing one

Figure 1.19: Scatter of various simultaneous measurements of the drag coefficient c_D and of the wind speed at 10 m height. The straight line is a regression line for the scatter. After De Cosmo et al. (1996).

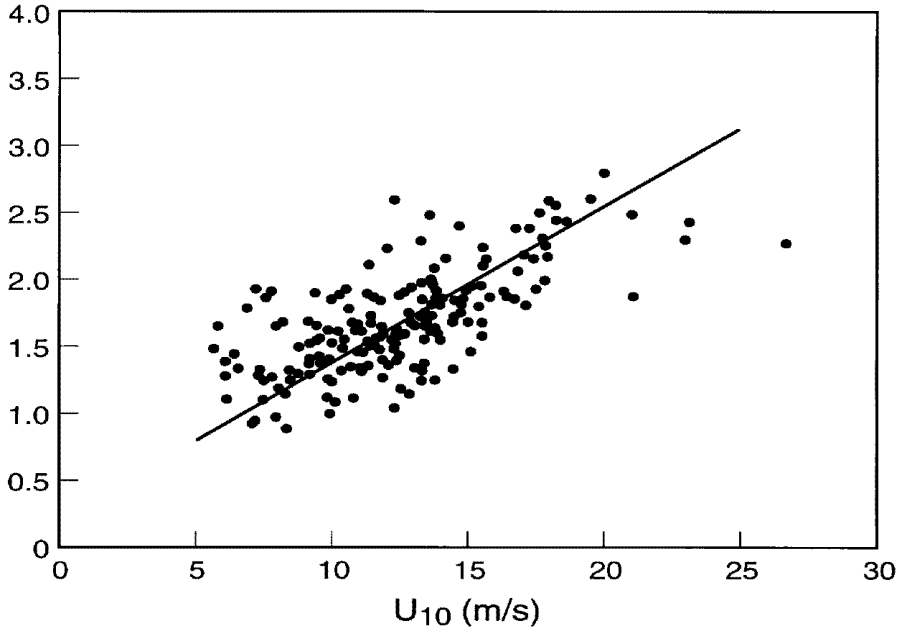

observation, and a summarizing regression line. Thus, to completely specify the parameterization (1.31), disregarding the dependency on the thermal stratification for the time being, the drag coefficient is specified as a linear function of $|\vec{u}_{10}|$, namely

$$\widehat{c_D} = a + b \cdot |\vec{u}_{10}| \tag{1.32}$$

where a and b are not relevant in the present discussion. This type of specification has been used in countless simulations with numerical ocean circulation models and ocean surface wave models forced with observed wind fields.

The question is what to do about the scatter around the regression line in Figure 1.19. The application of the bulk formula (1.31) with the regressed $\widehat{c_D}$ implies that the scatter is considered inconsequential or artificial, reflecting observational errors. The alternative interpretation is, however, that unknown processes (such as the sea state, gustiness of the wind, secondary flows) influence the value of c_D so that it exhibits unaccounted variations almost symmetrically around the regression line with a standard deviation of $\sigma \approx 0.5$ units. Therefore, a randomized version of the bulk formula (1.31)

Figure 1.20: Realization of randomized EBM
Top: time series;
Bottom: Frequency distribution of the temperature.

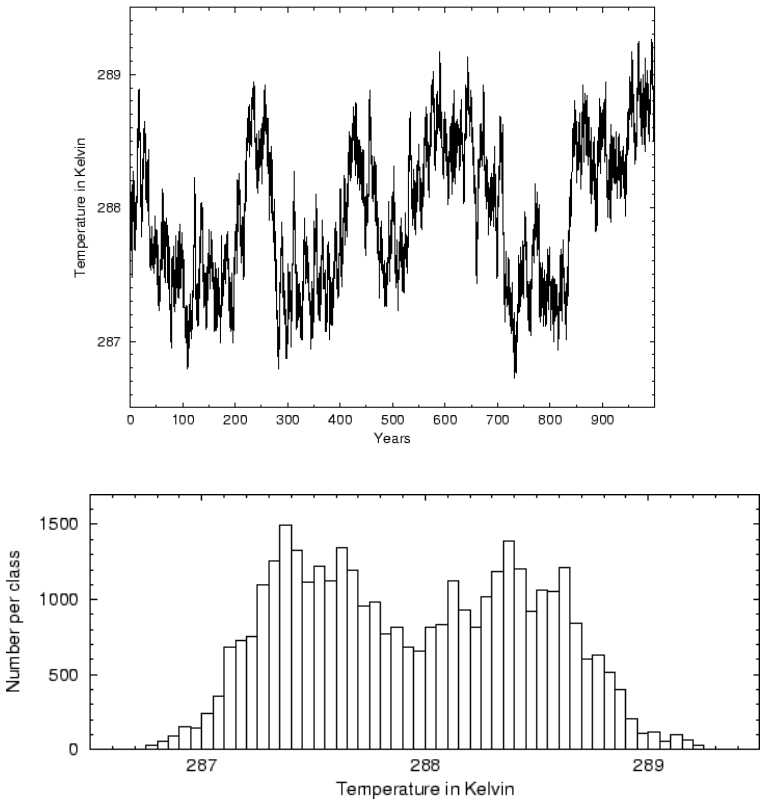

would use

$$c_D = \widehat{c_D} + \mathbf{N} \tag{1.33}$$

with

$$\mathbf{N} \sim \mathcal{N}(0, \sigma) \tag{1.34}$$

provided that the bulk formula is used with sufficiently large time steps so that the temporal correlation may be disregarded.

The question is, of course, if the use of the randomized parameterization (1.30) has an effect on the performance of the model in which the parameter-

ization is used. One may argue that the introduction of noise, represented by $\mathcal{S}$', is inconsequential since the contributions will just be averaged out. This may indeed be so in many cases, in particular in diffusive systems, but the situation is similar to the case of the *stochastic climate model* (Hasselmann, 1976), where the noise acts constructively in building red noise variance. We argue that the use of the randomized design (1.30) will enhance the variability of the considered model on all time scales, and will demonstrate this prospect by means of the energy balance model introduced in Section 1.2.

Differently from the deterministic model considered in Section 1.2, the process of long-wave radiation is not set to be constant, but it is randomized by adding a random term, with zero mean and a standard deviation of 3%:

$$\kappa = 0.64 + \mathbf{N} \tag{1.35}$$

with a random variable $\mathbf{N} \sim \mathcal{N}(0,\ 3\%)$ which may represent the effect of variable clouds and vegetation, for instance. The effect of this randomization on the global mean temperature $\bar{T}$ is shown in Figure 1.20.

Note that the resulting model itself has become a stochastic model, since it delivers a different path in its phase space for each simulation. Differently from the smooth convergence towards one of the stable equilibria in Figure 1.5, the trajectory performs an irregular wandering between two regimes, which correspond to the two stable equilibria of the non-randomized system. Overlaid are short-term erratic variations around these equilibria. The existence of the two statistical equilibria is documented clearly from the bimodal histogram of the temperature shown in the lower panel of Figure 1.20. Thus, the addition of noise transforms the simple dynamically inactive deterministic system into a much richer dynamically active system.

The noise does not act as a nuisance, or a veil blurring the dynamics of the system; instead, the noise contributes a significant component of the dynamical system. Therefore, it appears likely that the randomization of sub-grid scale parameterizations in numerical dynamical models will have an effect on the simulated space-time statistics; in particular, one may expect the overall level of variability to be enhanced and that more often transitions between different sub-regimes, if they exist, will occur. Also, the extreme values may become larger.

1.6 Epilogue

The major result of the present paper is that regional climates do not create the global climate. Instead, the regional climate should be understood as the result of an interplay between the global climate and the regional details. The local processes are important for the formation of the planetary climate, but not in terms of their details, only through their overall statistics.

This understanding has two important implications:

- It is possible to model the planetary scale climate with numerical models with limited, and even rather coarse, spatial and temporal resolutions of several hundred kilometers.

- The success of such models on the planetary scale implies by no means that such models are skillful in the simulation of regional and local features. [16]

Indeed, this dual fact has been noticed by weather forecasters already in the first half of our century, as is documented by Victor Starr's statement from 1942 :
"The general problem of forecasting weather conditions may be subdivided ... into two parts. In the first place, it is necessary to predict the state of motion of the atmosphere ... and, secondly, it is necessary to interpret this expected state of motion in terms of the actual weather which it will produce at various locations. The first of these problems is essentially of a dynamics nature ... The second problem involves a large number of details because, under exactly similar conditions of motion, different weather types may occur, depending upon the temperature of the air involved ... and a host of local influences."

In more modern terms, Starr's statement is that we can describe the large-scale climate dynamics well with our models, but that we need specific *downscaling* techniques to arrive at meaningful statements about the regional and local states. Indeed, the mathematics of modern downscaling techniques have their roots in the synoptic climatology and statistical techniques such as *Perfect Prog* which were developed already in the 1950s and 1960s.

However, since climate modeling is not merely an extension of weather forecasting, climatic evolutions on the small scale can not be completely described (or optimally guessed) by evolutions on the large-scale; instead, such local evolutions must be understood as being partially random in character. Therefore, parameterizations as well as weather generators, as opposed to local weather forecasts, should be randomized.

1.7 Acknowledgements

Stefan Güß supplied me with the EBM example. Enjoyable discussions with Peter Müller, Klaus Hasselmann and Kristina Katsaros helped clarify the concept of randomized parameterizations. Warren Washington helped with a review of the manuscript.

[16] The failure of GCMs in this respect was usually not explicitly mentioned, and non-specialist users of information provided by GCM data were unaware of this limitation. This caused sometimes bizarre situations, as for instance an analysis of the differences of climate change on the Northern and Southern slope of the Alps in a GCM too coarse to resolve the Alps.